PAPER • OPEN ACCESS

Detailed CFD transient heat transfer modelling in a brake friction system

To cite this article: Francesco Orlandi *et al* 2022 *J. Phys.: Conf. Ser.* **2385** 012030

View the article online for updates and enhancements.

Detailed CFD transient heat transfer modelling in a brake friction system

Francesco Orlandi

DISMI - dept. of sciences and methods for engineering University of Modena and Reggio Emilia, Reggio Emilia, IT

E-mail: `francesco.orlandi@unimore.it`

Massimo Milani

DISMI - dept. of sciences and methods for engineering University of Modena and Reggio Emilia, – Centro InterMech MO.RE., Reggio Emilia, IT

E-mail: `massimo.milani@unimore.it`

Luca Montorsi

DISMI - dept. of sciences and methods for engineering University of Modena and Reggio Emilia, – Centro InterMech MO.RE., Reggio Emilia, IT

E-mail: `luca.montorsi@unimore.it`

Abstract. In a brake system the contact between the friction grooves of the discs and the steel elements leads to a consistent heat dissipation that is excised by the oil thermal vector in its flowing along the grooves channels. These are very complicated physical system were many variables may be taken in consideration, first of all the extensive integration of the different time scheduling actions that take place and that characterizes the translation of the interacting bodies and the correspondent deceleration, and also the heat dissipation derived from this contact. The simulations of similar physical system may result in too expensive computational efforts leading to very complicated simulations that need to take in account an extensive coupling between many physics, first of all the solid/liquid heat transfer and then the turbulence and the bi-phase models for the oil/air mixture that serves as thermal refrigerator vector in the braking system. Herein a simplified 3D model that focuses only on a discs / piston coupling is presented were the braking action is simulated in a simplified way modelling the velocity of rotation of the elements and the dissipated heat during the braking cycle. Focusing on the grooves channels the oil flows and thermal averaged flows are presented and detail contours are used to characterise a single brake event.

1. Introduction

A discs braking system is a device that is used to force the stop of a generic vehicle, and exist many configurations of this technology. Focusing on a tractor brake system it is constituted by two or more friction discs splined to the rotating shaft, which transmits the torque to the rotating components and the reducer to the wheels, and steel elements, called separators, pivoted in the housing and splined by the contact with the friction elements once the braking happens. The friction discs themselves are generally constituted of an extruded pattern, that can be of

different forms, made of a friction material characterized by low conductivity, bonded on a steel
support which is splined with the rotating shaft, that also aids oil flow from the inner edge
of the plate to the outer edge. During the braking event, the piston is pushed in contact by
means of an oil circuit pressure ramp with the friction disc and the relative rotation between
the rotating friction discs and the static steel elements leads to a progressive slowing down of
the rotating components until the complete rest of the system is reached. The contact friction
between the steel and the frictions components releases high amount of energy in the system
that is dissipated under the form of thermal energy. The use of lubricating oil that is put in
motion by the rotation of the discs and fills the discs chamber in an air/oil mixture, constantly
injected in the discs chamber, flowing through the surfaces of the friction discs and steel plates,
enhances the efficiency of the brake system, dissipating the heat within the components and
reducing the wear behavior.

In literature the most of the studies have been done regarding clutch systems, that in more
than a way represent a very similar topic to the one of the braking systems. In both the systems
there is a coupling between rotating and non rotating elements and a disengage/engage that
leads to high power dissipation due to relative rotation and friction between the elements in
contact. Lot of studies were performed to find relations during the disengage event and the
torque calculation also with means of analytic studies ([1],[2],[3],[4],[5],[6],[7]). Unfortunately,
the analytic approach results in good agreement with the measurements only for simplified ge-
ometries, while for more complex geometries like the realistic grooves patterns of the rotating
discs deviations are obtained from the test measurements.
Obviously also the numerical approach needs to account for simplifications and the reliability
of the results depends much on the simplifying hypothesis applied on the single case of study.
Mainly executed with means of Simcenter STAR-CCM+ and ANSYS mainly, the simplest stud-
ies generally involve single phase models ([8],[9]), but doing so the lubricating oil distribution
tend to lead to over simplistic results while the temperature field distribution gives generally
good agreement with the experiments. More accurate studies were realized considering two-
phase models ([10],[11],[12],[13],[7]) of the oil/air mixture, implementing the Volume of Fluid
method mainly. Then, most of the current studies focus mainly on single discs analysis or single
steel-disc coupling ([14],[15],[16],[17],[18]), where the influence of the different geometric pattern
was demonstrated to be a fundamental parameter ([19],[20],[21]) , while few exist that investi-
gated more elaborated geometries ([22],[23],[24]).
With the studies operated on the clutches is possible in the end to use all this methodologies
to study the braking systems, that as written before is a specular system working under similar
physic conditions, but with the main mechanism that is inverse, so the engaging between the
elements that leads to the deceleration of te system until its rest. So if the clutch system trans-
mits motion the braking system obstacles the motion. From this some studies were performed
in transient 3D simulations ([25],[26]).
In the present study the simulation of a braking event focused on the heat dissipation in the
fluid domain in between of the steel and friction plate region was carried on in Simcenter STAR-
CCM+. The braking event was simulated by means of trends of the rotation velocities and of
the dissipated heat fluxes from the steel and the friction materials, extrapolated by literature
relations, and applied to the respective surfaces of interest.

2. Physic Continuum
For the present simulation of a braking killer test event a 3D CFD simulation was developed in
Simcenter STAR-CCM+ environment [27]. The two-phase oil/air fluid mixture was modelled
with means of a VOF model [28], where the single phase f is tracked by means of a color function

$$C_i = \frac{1}{V_i} \int_{V_i} f\left(\overline{x}, t\right) dV,\tag{1}$$

so that in the end the color function itself can be associated with the single reference phase

$$C_i = \frac{V_i}{V},\tag{2}$$

defined as a volumetric fraction. The oil/air mixture was modelled as an incompressible fluid leading to the well known Navier-Stokes equations system

$$\frac{\partial \rho_i}{\partial t} + \nabla \cdot (\rho_i \overline{u}_i) = 0\tag{3}$$

$$\frac{\partial \rho_i}{\partial t} + \nabla \cdot (\rho_i \overline{u}_i) = \rho_i g - \nabla p_i + \nabla \tau_i\tag{4}$$

where the i subscript identifies the single phase. Since in the braking event energy is dissipated in the system in the form of thermal dissipation due to the friction between the element, the energy equation was implemented too

$$\frac{\partial \rho_i E_i}{\partial t} + \rho_i \nabla \cdot (E_i \overline{u}_i) = -\nabla \cdot p_i + \nabla \cdot (T\,\overline{u}_i) - \nabla \cdot q + S\tag{5}$$

The oil phase was characterized by means of field functions, customizable macro in the software environment, based on the MultiG industrial oil characteristics, while air was kept at the library values already available in the software library. Since the braking systems are characterized by high velocities of rotation of the shaft, a turbulent model is necessary to properly model the fluid motion. Considering the narrow sections of the grooves channels in the friction part of the discs, the choice fell upon the use of a Menter's $\kappa - \omega\,SST$ formulation [29] due to its capacity to handle little sections as the Wilcox's $\kappa - \omega$ (Wilcox) and the blending with a $\kappa - \epsilon$ [30] turbulence model in the sections that result distant from the walls, which is defined as

$$\frac{\partial \rho \kappa}{\partial t} + \nabla \cdot (\rho \kappa \overline{u}) = \nabla \cdot \left[\left(\mu + \frac{\mu_t}{\sigma_\kappa}\right)\right] + P_\kappa - \rho\left(\epsilon - \epsilon_0\right) + S_\kappa\tag{6}$$

$$\frac{\partial \rho \epsilon}{\partial t} + \nabla \cdot (\rho \epsilon \overline{u}) = \nabla \cdot \left[\left(\mu + \frac{\mu_t}{\sigma_\epsilon}\right)\right] + \frac{1}{T_e}C_{\epsilon 1}P_\epsilon - f_2\rho\left(\frac{\epsilon}{T_e} - \frac{\epsilon_0}{T_0}\right) + S_\epsilon\tag{7}$$
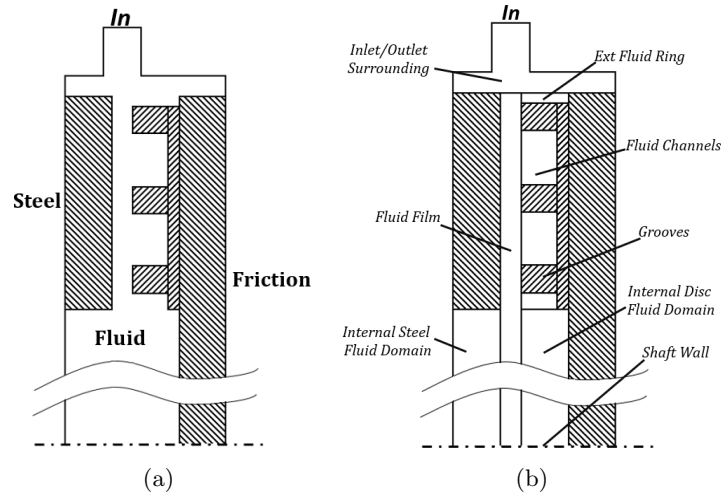
3. Geometry

Figure 1: *(a) Reduced Brake Geometry Scheme and (b) friction disc fluid domain separated regions*

The analyzed system is a simplified braking system constituted by a friction/steel couple. Starting from a 3D braking steel/friction elements couple the system was simplified in order to focus only on the steel/friction elements coupling as in Fig. 1a. The braking disc is constituted by a steel support and a friction material pattern (generally named grooves) bonded on the support. Since the study focuses on the thermal energy dissipation in the grooves channels of the friction disc the friction disc geometry was reduced to one single side that extends to the steel surface support. The same depth of the friction fluid domain was reproduced in the steel fluid domain. The surroundings, that in the complete real geometry of the braking system correspond to the discs chamber, the inlet and the outlet channels, were simplified in an external fluid ring surrounding the solid steel/friction elements and the channels of the inlet and outlet where substituted with two channels directed along the axis of the fluid film that separates the steel element and the friction element. The physic domain in the present study is constituted of only fluid. Fig. 1b shows the subdivision of the geometry in regions since they will be meshed independently. As shown in Fig. 1b the fluid domain can be divided, in order to handle the mesh with higher precision, into 4 different regions. These regions are namely the inlet/outlet region and the inner regions. The inlet/outlet regions are comprised of the two cylinder-like shape for the inlet and the outlet pipe and an external ring surrounding the inner regions, as in the above part of Fig. 1b. The inner regions are the internal steel domain, the fluid film and the friction disc domain, which is comprised of all the regions on the right corresponding to the parts constituting the friction disc fluid domain, as in Fig. 1b. The latter was further divided in three other distinct regions, being the external fluid ring, the fluid channel and the internal disc fluid domain. This operation lets the operator to parameterize the mesh with more accuracy, where the connections between the different meshes will be simply managed by static interfaces.

4. Mesh
The mesh generation made use of two distinct methods both available in Simcenter STAR-CCM+ environment. For the friction's fluid, fluid film and the steel fluid regions a directed quadrilateral mesh was used. This method permits to generate high quality swept meshes by sweeping a mesh from the surfaces of a source geometry through its volume onto a facing target

surface. The control over the sweeping gives the possibility to generate high quality meshes with an economy onto the computational weight of the mesh itself. In Fig. 2a a detail of the friction channels is shown. The use of the quadrilateral directed mesh can be see to generate a regular subdivision of the narrow channels of 2e-3m, and with the dimension chosen, as reported in Table 1, 5 cells were generated into the channels. The depth of the channels being 8.5e-4m led to the choice of 8 layers in order to have the necessary mesh precision along with the avoiding of generating too stirred cells. In Fig. 2b an overall portion of the fluid film meshed region is shown, and a detail of the volume layers is reported. Regarding the inlet/outlet region an automated mesh was chosen, where no volume sweeping must be set and the software itself manages the most of the mesh. This was chosen so since no particular requirements are necessary outside of the steel/friction element regions, in facts the base size was chosen as the bigger in confront to the other regions as reported in Table 1.

Table 1: *Mesh Parameters*

Region	Mesh	Base Size	Volume Layers	Prism Layers	Cells Number
Friction	directed quad	2.5 e-4m	8	-	1551342
Steel	directed quad	5 e-3m	8	6.25e-4	799854
Fluid Film	directed quad	2.5 e-3m	4	3.125e-4m	73745
Inlet/Outlet	automated poly	5 e-3m	-	1.56 e-4m	164857

To simulate the braking event, as it will be further described in detail, no 3D rotation of the rotating region was performed. A wall relative condition was set in all the surfaces of the disc's fluid domain, that is the only element which is integral with the shaft that transmits the rotation, and in the fluid film and steel fluid regions along the perimeter of the shaft walls, as it can be seen on the left of Fig. 2b. The wall relative rotation, along with the turbulent characteristics of a brake system, led to the necessity of the implementation of a prism layer. This was characterized by a thickness value set with means of a fixed relative percentage in respect to the base size. This led to different values in the regions where it was set (a part from the Inlet/Outlet region where the value was chosen accordingly to the narrower sections). The values were considered correct if they respected the y+ values required by the All Y+ Wall Treatment. This wall treatment blends a wall function that works under low y+ values (~ 1) for fine meshes and over high y+ values (>30) for coarser meshes. For the rotating discs' walls the refinement of the mesh was such that the y+ dimension respected the low y+ condition and was no necessary to define any prism layer.

(a) Grooves Channels detail

(b) Disc/Steel Leakage detail
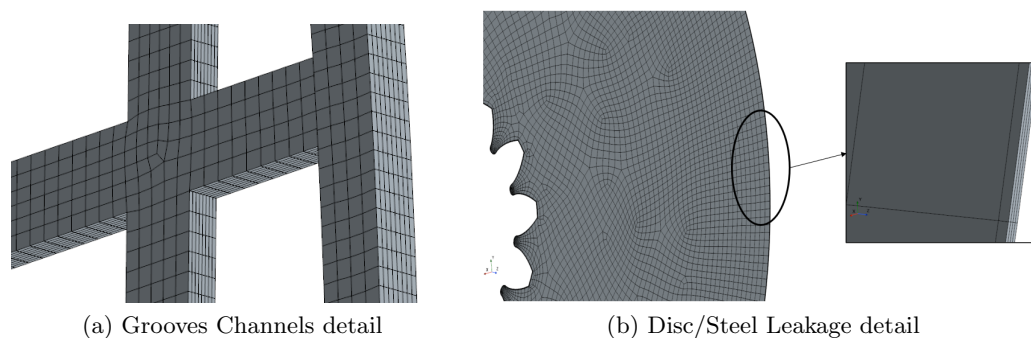
Figure 2: *Mesh detail*
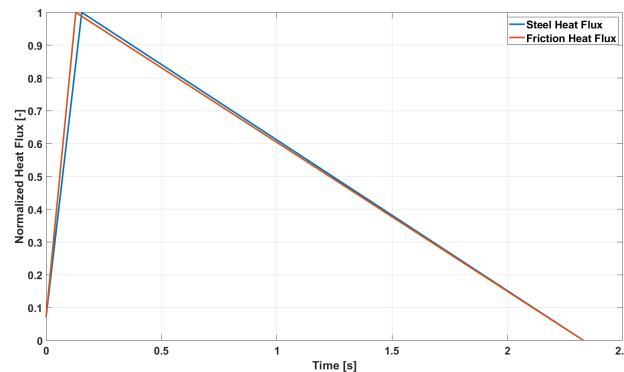
5. Simulation Settings

Figure 3: *Brake event normalized heat fluxes (a) orange for the friction disc and (b) blue for the steel component*

In the present study a brake killer test, based upon the standard procedure for a middle weight tractor manifacture, was simulated. Each brake action is followed by the subsequent after a period of 45s. Fig. 3 shows the normalized heat flux released into the fluid domain surroundings based on a real tractor brake system experimental results. The trends were obtained from an existent relationship [4] where the dissipated thermal energy released from the friction contact between the friction and the steel plates is obtained. From [4] a defined ratio between the thermal dissipated energy of the steel plate and the friction can be obtained. The resulting curve has been adapted to the experimental results by interpolations on time and heat flux values in order to maintain the area underneath the curves fixed as obtained from the original literature source. Doing so the cumulative dissipated energy equals the total value at the end of the dissipation event. Also, the ratio between the steel and friction heat fluxes remains unaltered. Since no solid components are included in this study the heat fluxes in Fig. 3 are released directly to the surrounding fluid that wets the channels, the steel plate walls and the fluid film. In order to do so, the correspondent steel/friction heat fluxes values were specified in the static fluid interfaces interested during the dissipation period.
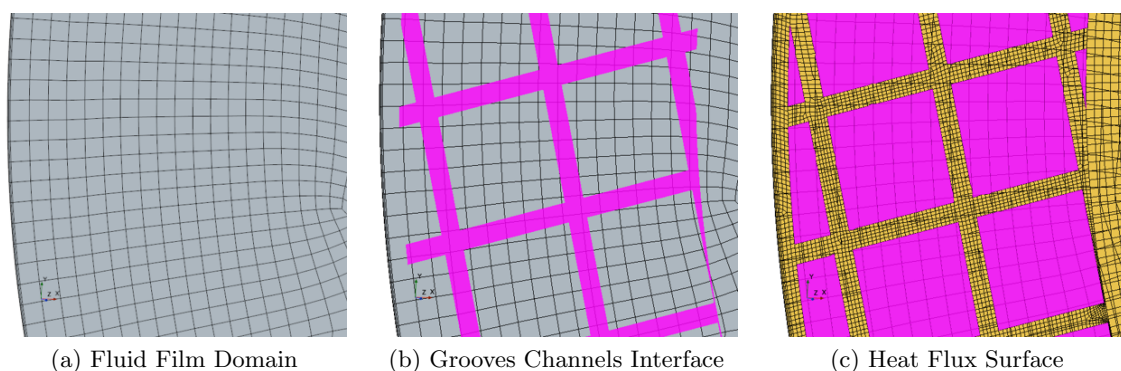

(a) Fluid Film Domain   (b) Grooves Channels Interface   (c) Heat Flux Surface

Figure 4: *Friction heat flux surface details*

Fig. 4 shows the progression during the definition of the interface between the fluid channels and the neighbor fluid film region. The definition of the heat fluxes took advantage of the interface generation between the fluid film region and the neighbor regions, namely the disc and

the steel fluid domain. As shown in Fig. 4 the generation of the interfaces between the disc and the fluid film region (in Fig. 4 only the channels interface is shown as an example) leads to the remaining free surface in Fig. 4c. This overall surface is the exact mirroring of the grooves head so the heat flux release was set in this fluid region, leading to a precise miming of the real region responsible for the heat dissipation. The same procedure hold for the steel region.
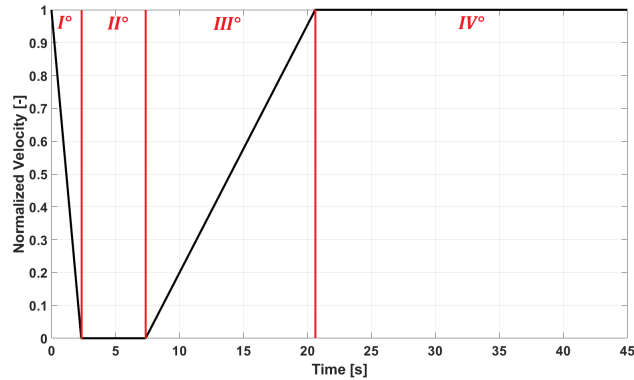

Figure 5: *Brake event normalized velocity profile*

The second trend that needs to be implemented is the velocity profile, that reproduces the steps that follow to a brake event. These steps are the deceleration of the plates following the pushing to contact of the piston by the oil pressure rising, the rest period where the plates are still in contact before the pressure decrease onto the piston,the acceleration ramp and the nominal velocity period where the shaft reaches back the full velocity rotation. In Fig. 5 the described velocity profile is reported, and for clarity it has been listed in the following:

- I Dissipation period: the friction element and the steel element get in contact and thermal energy is released in the system for dissipation phenomenon due to the friction contact between the elements.
- II Rest period: the braking is complete and the elements are still.
- III Acceleration period: the shaft starts to accelerate until the nominal velocity is reached.
- IV Nominal period: once the nominal velocity is reached it is mantained for some seconds until a new braking event is performed.

Obviously the trend reported in Fig. 5 is referred to the relative wall rotation, and no axial movement of the elements was simulated. This means that the simulated braking action does not include the contact between the elements, so the clearance between the steel and the friction element is not modified during the calculation. The trends reported in Fig. 3 and Fig. 5 were implemented by means of a .csv table constituted of two colums, time and the respective quantity. These tables were linearly interpolated so that the original trends were simplified neglecting the small variations that follow from the experimental tests. In order to move the oil in the chamber, wall relative rotations were set at the desired boundaries, i.e. the shaft perimeter and all the boundary surfaces of the friction disc fluid domain. The initial condition for the simulation was defined as the system at rest and half filled by oil in the lower middle part and air in the upper middle part. The mass flow inlet was set accordingly to the values of the experimental tests and the outlet was set as a pressure outlet, where a constant piezometric contribution was added to the pressure at the outlet so that $p = \rho_{ref} g (x_0 - x)$, with ρ_{ref} is the reference density of the oil, g the well known gravity acceleration, x and x_0 the altitude and the reference altitude. In a real braking system the pressure outlet would have to be defined with varying values since the working of the differential gear adiacent to the gears chamber

influences the outflow of the lubricating oil. This means that depending on what happens to the boundary conditions of the differential gear chamber the pressure values at the outlet of the discs chamber change accordingly. For the present study a simplified condition with a constant outlet pressure greater than the reference pressure was set, adding the contribution of the oil column upon the pressure outlet with the hypothesis that in a complete mixing of the oil the piezometric contribution to the outlets doesn't change.
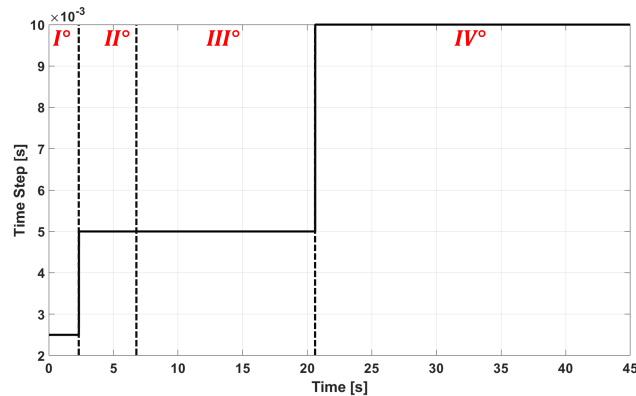

Figure 6: *Brake event time steps*

To increase the precision of the simulation, and taking in count the different events that characterize a single cycle, three different time steps values were used in the simulation. Fig. 6 shows the three different time steps magnitude and the periods of interest of the simulation. A finer time step value of 2.5e-3s was used during the dissipation event, where the temperature gradient and the sudden decrease of velocity lead to strong instabilities for the calculation, then the time step increases to 5e-3s during the rest and the acceleration period and finally during the nominal velocity period it was risen to value of 1e-2s. This procedure was conceived in order to speed up the simulation taking advantage of the existence of only one effective critical period being the dissipation one, where the other cycles only deal with the convective diffusion of the thermal energy through the air/oil mixture without a source term.

Five braking tests have been operated after a full velocity period without braking action of the system where the fluid-dynamic conditions of statistical stability were reached. The number of the braking cycles were chosen in order to obtain the thermodynamic and fluid-dynamic stability of the physic domain, that was reached at the Vth braking cycle.

6. Results

The results of the Vth braking cycle are reported. First, temperature field contour plots are shown within a section passing by the middle of the grooves height. Each contour plot is reported at a different time step, chose in order to give a good overview of the dissipation period. In the same section, oil volume fraction contour plots are shown at the same time steps. Oil volume flow trend in the grooves channels and the mass-flow average temperature flows in the grooves channels are then reported.

Fig. 7 shows the temperature field in a section, positioned in the middle of the depth of the grooves of the friction disc. Three different time frames are here reported, specifically the immediate beginning of the braking action, the middle of the dissipation cycle, i.e. I in Fig. 5, and the end of the dissipation cycle. In (A) an initial average temperature rising appears in the channels for values of approximately 200°C, while the mean temperature values in the external ring remains substantially unaltered and the internal temperature field shows an increase flowing
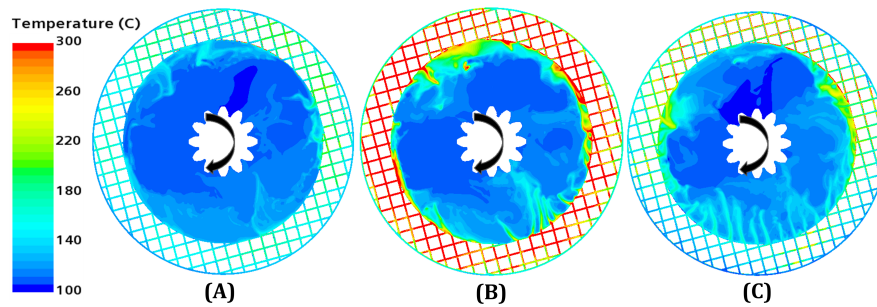
Figure 7: *Temperature field along the channels section of the friction disc during (A) Beginning of the Braking Cycle, (B) Middle Dissipation Event, (C) End of the Braking Action*

from the channels of hot flows of approximately 150°C. With the progress of the dissipation cycle in (B) the average temperature rises to 300°C in the channels region and a reducing velocity effect is observable. This effect, that acts mainly on the distribution of oil is highlighted by the temperature diffusion in the internal region of the disc fluid domain. Here the oil flows out from the channels to the internal region due to the discs slowdown and the consequently decrease of the centrifugal force. In (C) the braking action has reached its end, so the rotating components are at rest. The overall temperature is decreased in comparison to (B), due to two main factors that are the continuing flowing of lubricating oil and the decreasing in dissipated energy as shown in Fig. 3. In (C) the temperature in the channels has further decreased. In the upper part of the channels and in correspondence of the walls perimeter is still possible to find some residuals of higher temperatures around 300°C. In the other channels sections then the temperature shows average values in between of 250°C and 150°C. The lowest temperatures are found in the external ring below the middle plane of the disc fluid domain.

Fig. 9 shows the mass flow average temperature of the oil/air mixture flowing through the channels. The flows that characterize the channels are schematically shown in Fig. 8 and are basically three:

- The oil pushed outside of the channels in the direction of the external ring due to the centrifugal force during the normal functioning of the tractor. In red, named External Flow and positive when flowing outside of the channels.

- The oil that is pushed into the channels by means of the centrifugal force from the internal fluid region of the disc. In green, named Internal Flow and positive when flowing outside of the channels.

- The oil that flows outside of the channels in the normal direction to the surface. In blue, named Out Flow and positive when directed outside of the channels.

Figure 8: *Channels Flows Schematic*

In Fig. 9 the mass flow averaged temperature fields of the three different flows in Fig. 8 are shown. The external flow is the one that reaches the averaged lower values, with an average peak of 210°C and decreasing to 130°C at II, i.e. at the end of the braking action. The internal flow follows with an higher peak of 292.5°C and a decrease to 170°C at II. The higher averaged temperature values are reached by the out flow with a peak value of 345°C and a value at II of 180°C. It is also interesting to observe that the higher temperature values for the three flows differ in time. This is due to the different mixing of the oil/air mixture with the surroundings. After the braking action the outflow and the external flow show a similar trend with an initial increase in temperature and a decrease in correspondence to the IV subcycle, i.e. constant nominal velocity, in the order of 20°C for the outflow and 10°C for the external flow.
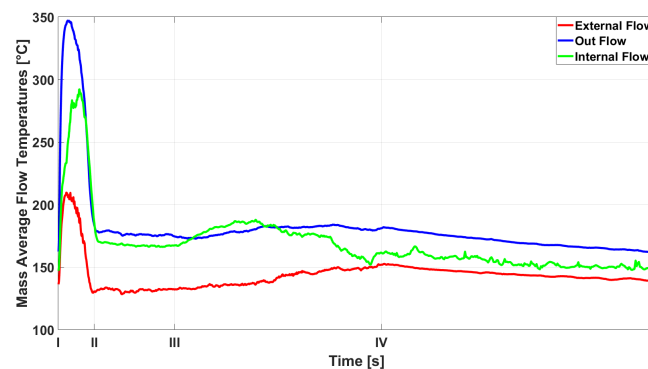

Figure 9: *Mass Flow Averaged Temperatures in the grooves channels*

The internal flow then shows a different trend with an intense decrease that starts after the middle of the acceleration ramp and continues with a less steep trend when the nominal velocity is reached. This trend of the internal flow is easily explained considering the higher mixing that characterizes the fluid domain in correspondence of the internal diameter due to the higher mixing space at disposal. In the channels region and the outlet ring then the narrower passages hinder an efficient mixing of the oil/air mixture.

Fig. 10 shows the oil volume fraction contour plots during the braking steps as in Fig. 7. In all the three frames the stratification of the oil/air mixture is evident. Also, the effect of the braking action is highlighted by the increasing in oil concentration on the bottom of the section. In the reported sections the higher concentration of oil in the bottom, with an high value already detectable in (A), shows that the wall relative rotation is not sufficient to drag the fluid with enough force to put it in motion in its entirety. It is in fact important to remember that the shown braking results are referring to the fifth cycle in series. This means that in (A) the fluid has experienced the nominal velocity period of the preceding cycle, and it would be expected that it would be more mixed with an average value of oil/air quite regular in the whole fluid domain here reported.
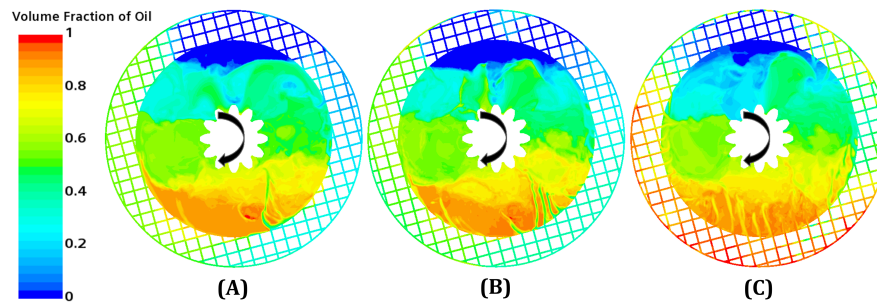
Figure 10: *Oil Volume Fration along the channels section of the friction disc during (A) Beginning of the Braking Cycle, (B) Middle Dissipation Event, (C) End of the Braking Action*

In Fig. 11 the volume flows as reported in Fig. 8 are shown. The dynamic of the braking of Fig. 5 is clearly highlighted by the subdivisions and the fluid dynamic faithfully follows the braking action operative velocities. The first dissipation period, that corresponds to the decreasing in velocity until the rotation is completely stopped, leads to a negative average value for the external flow and the opposite in an increase in positive values for the internal flow. This depends on the decreasing of the centrifugal flow that follows to the deceleration of the rotating components that makes the oil/air mixture to flow through the channels from the surrounding fluid ring. Consequently this leads to an increase of the flowing from the channels to the internal region of the disc fluid domain. Regarding the out flow, during the dissipation period the flow averagely inverts the sign leading to an average flowing of the oil/air mixture towards the channels from the adiacent fluid film region. Within the rest period the trends tend to invert the direction and decrease in module. Within the acceleration ramp this trend grows quickly until the nominal velocity period where the values tend to settle to a fixed average value. The main result here has to be linked to the wall relative rotation as in Fig. 10. Differently from the internal flow, the external flow inverts the trend in module of the average volume flows but it never changes in sign. This means that averaging the external flow is negative, i.e. flows inside of the channels. Apparently this could be interpreted as an error since starting with the acceleration ramp the centrifugal force increases and the oil is radially pushed through the channels from the inside region to the surrounding regions. The internal flow then clearly shows that the direction is inverted and with the acceleration ramp it starts to being pushed through the channels by means of the centrifugal force. It has to be remembered that the reported values are referred to average values along the interfaces of the different regions with the channels. This means that the average external flow mainly flows back into the channels from the outside ring, probably due to the high concentration at the bottom of the oil phase as in Fig. 10. Then, this doesn't mean that the external flow doesn't ever proceed in the correct manner being pushed outside of the channels with the increase of the relative wall rotation.

7. Conclusions

In the present work a 3D transient simulation model was presented, which enables the calculation of the energy dissipation into the lubricating oil fluid in a single brake steel/friction couple configuration, based on a standard braking killer test for tractors machine of medium weight. The model is characterized by the followings

- The heterogeneous phase distribution was modeled by means of a Volume of Fluid method.
- The 3D rotation of the friction disc was neglected and a wall relative rotation was implemented instead.
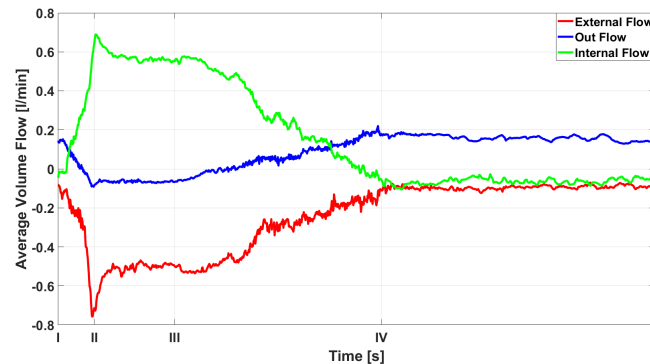
Figure 11: *Average Volume Flow in the grooves channels*

- The braking action was simulated by means of a relative wall rotation profile and an heat flux profile released at the interfaces of the regions involved in the braking action. To speed up the solution a three level time step was implemented.

Contour plots for the temperature field were reported for the main steps of the dissipation period of the braking cycle. These showed the increment of the temperature in the grooves channels of the friction part of the disc and the subsequent diffusion of the temperature. The diffusion phenomenon led to lower average temperatures, while higher values remain confined to the channels wall perimeter. A temperature line plot was then used to monitor the mass average flow temperature of the flows that interest the flowing in the channels. The temperature trend follow an increase during the first half of the dissipation period followed by a quick decrease and a stabilization of the average temperature. Oil Volume Fraction contour plots were shown during the three steps of the dissipation period and showed that the drag of the oil is not sufficient to put in motion all the oil fluid. The residual amount of oil that remains confined in the lower section demonstrates that an average drag and movement of oil takes place but a 3D rotation is necessary to avoid such stagnant quantity of liquid phase. The line plot of the average channels flow reported the same phenomenon. In fact for all the braking event the external flow remains negative on average due to the high oil concentration in the depot point in the lower part of the disc region. The outflow and the internal flow then invert their values during the dissipation period and from the rest period to the nominal velocity period return to their original trends. In the future this numerical model can be applied to a more extended geometry and more realistic inlet/outlet channels. Also, a 3D rotation can be implemented to verify the differences in the heat diffusion due to the complete drag of the oil .

References

[1] Jang J Y and Khonsari M M 1999 *Journal of Tribology* **121** 610–617 ISSN 15288897
[2] Iqbal S, Al-Bender F, Pluymers B and Desmet W 2013 *ISRN Tribology* **2013** 1–16
[3] Pahlovy S, Mahmud S F, Kubota M, Ogawa M and Takakura N 2014 *SAE International Journal of Commercial Vehicles* **7** 441–447 ISSN 1946-391X URL https://www.sae.org/publications/technical-papers/content/2014-01-2333/
[4] Zhigang Z, Xiaohui S and Dong G 2016 *Mathematical Problems in Engineering* **2016** ISSN 15635147
[5] Pahlovy S A, Mahmud S, Kubota M, Ogawa M and Takakura N 2017 *SAE Technical Papers* **2017-March** ISSN 0148-7191 URL https://www.sae.org/publications/technical-papers/content/2017-01-1132/
[6] Vasca F, Iannelli L, Senatore A and Scafati M T 2008 *Proceedings of the American Control Conference* 306–311 ISSN 07431619
[7] Peng Z and Yuan S 2019 *Chinese Journal of Mechanical Engineering (English Edition)* **32** ISSN 21928258 URL https://doi.org/10.1186/s10033-019-0343-9

[8] Huang J H, Fan Y R, Qiu M X and Fang W M 2012 *Journal of Central South University 2012 19:2* **19** 347–356 ISSN 2227-5223 URL https://link.springer.com/article/10.1007/s11771-012-1011-8

[9] Aphale C R, Cho J, Schultz W W, Ceccio S L, Yoshioka T and Hiraki H 2006 *Journal of Tribology* **128** 422–430 ISSN 07424787

[10] Aphale C R, Schultz W W and Ceccio S L 2011 *Journal of Tribology* **133** 1–7 ISSN 07424787

[11] Mahmud S F, Pahlovy S A, Kubota M, Ogawa M and Takakura N 2015 *SAE Technical Papers*

[12] Wu W, Xiong Z, Hu J and Yuan S 2015 *International Journal of Heat and Mass Transfer* **91** 293–301 ISSN 00179310 URL http://dx.doi.org/10.1016/j.ijheatmasstransfer.2015.07.092

[13] Wang P, Katopodes N and Fujii Y 2017 *SAE International Journal of Engines* **10** 1327–1337 ISSN 19463944

[14] Kitabayashi H, Li C Y and Hiraki H 2003 *SAE Technical Papers* ISSN 0148-7191 URL https://www.sae.org/publications/technical-papers/content/2003-01-1973/

[15] Neupert T and Bartel D 2015 *Getriebe aktuell* **5**

[16] Takagi Y, Nakata H, Okano Y, Miyagawa M and Katayama N 2011 *Journal of Advances Research in Physics* **2** 1–5

[17] Hu J, Peng Z and Wei C 2012 *Journal of Tribology* **134** 1–6 ISSN 07424787

[18] Cui H, Yao S, Yan Q, Feng S and Liu Q 2014 *Chinese Journal of Mechanical Engineering 2014 27:1* **27** 32–40 ISSN 2192-8258 URL https://link.springer.com/articles/10.3901/CJME.2014.01.032https://link.springer.com/article/10.3901/CJME.2014.01.032

[19] Qu D, Zhao C, Li X and Zhang C 2017 **71** 740–743

[20] Li M, Khonsari M M, McCarthy D M and Lundin J 2017 *Proceedings of the Institution of Mechanical Engineers, Part J: Journal of Engineering Tribology* **231** 1056–1067 ISSN 2041305X

[21] Yashwanth B L, Ngo D, Schroeder D, Hopson B and Wang D M 2018 *SAE Technical Papers* **2018-April** ISSN 01487191

[22] Bassi A, Milani M, Montorsi L and Terzi S 2016 *SAE International Journal of Commercial Vehicles* **9** 280–290 ISSN 19463928

[23] Terzi S, Manhartsgruber B, Milani M and Montorsi L 2018 *SAE Technical Papers* **2018-Septe** 1–11 ISSN 01487191

[24] Terzi S, Milani M, Montorsi L and Manhartsgruber B 2018 *Green Energy and Technology* vol 0 (IEEE) pp 89–111 ISBN 9781538647851 URL http://link.springer.com/10.1007/978-3-319-62199-9_4

[25] Singh S K, Abbassi H and Tamamidis P 2018 *Applied Thermal Engineering* **136** 576–588 ISSN 13594311 URL https://doi.org/10.1016/j.applthermaleng.2018.01.004

[26] Milani M, Montorsi L, Muzzioli G, Storchi G, Terzi S, Rinaldi P P and Stefani M 2020 *ASME International Mechanical Engineering Congress and Exposition, Proceedings (IMECE)* **10** 1–7

[27] Siemens PLM Software 2022 Star-CCM+ 17.02.007 User Guide

[28] Menter F R 2000 URL https://publikationen.bibliothek.kit.edu/3122000

[29] Menter F R 1994 *AIAA Journal* **32** 1598–1605 ISSN 0001-1452

[30] Launder B E and Spalding D B 1974 *Computer Methods in Applied Mechanics and Engineering* **3** 269–289 ISSN 0045-7825